



Modal identification of a small-scale ducted fan

A. Pereira*, E. Salze† and P. Souchotte‡

École Centrale de Lyon

Laboratoire de Mécanique des Fluides et d'Acoustique, UMR CNRS 5509

36, avenue Guy de Collongue, 69134 Écully, France

A. Finez§

MicrodB/Vibratec

28 Chemin du petit bois, Écully, 69134, France

Q. Leclère¶

INSA de Lyon, Laboratoire Vibrations Acoustique

25 bis avenue Jean Capelle, F-69621, Villeurbanne Cedex, France

The subject of this paper is the experimental investigation of the noise radiated by a ducted rotating machine. A modal identification approach is used to decompose the radiated sound field into duct modes from acoustic pressure measured by wall-flush mounted microphones. Both azimuthal and radial decompositions are computed by means of an array with optimized microphone arrangement. The optimized array ensures a low condition number of the matrix relating modal coefficients to acoustic pressure over a wide frequency band, up to the second harmonic of the blade passing frequency. Above this frequency the number of cut-on modes is comparable to the number of microphones and the modal matrix suffers from ill-conditioning. A regularization procedure is then introduced to increase the high-frequency limit of the method. Results are presented for both tonal and broadband components of the radiated sound field. The difficulty in the broadband regime is that pressure fluctuations measured by in-duct microphones are strongly affected by hydrodynamic noise associated to the turbulent boundary layer (TBL). A technique to suppress the TBL related noise is thus applied prior to the modal identification, its interest is shown on experimental data from an academic test bench.

I. Introduction

THE investigation of noise generation mechanisms from turbomachinery is a current problem in aeroacoustics. Several approaches, either analytical,¹⁻³ numerical or experimental⁴⁻⁷ have been proposed in this context. The interest in this paper is the experimental characterization of a ducted fan system based on microphone array measurements. In this context two different approaches with respect to the microphone array configuration may be distinguished: (i) a first one in which the microphones are installed outside the fan inlet, in the near field; (ii) and a second one in which microphones are placed flush-mounted on the duct inner surface. The advantage of an external microphone array is that measurements are less perturbed by the hydrodynamic noise (associated to the turbulent boundary layer (TBL)) and thus modal decomposition may be readily applicable to both tonal and broadband components. One difficulty, however, is that the propagation model relating measurements to modal amplitudes may not be available analytically and one has to resort to numerical models⁵ of the radiated field. This approach has been addressed by Castres et

*Postdoctoral Researcher, antonio.pereira@ec-lyon.fr

†Research Engineer, edouard.salze@ec-lyon.fr

‡Research Engineer, pascal.souchotte@ec-lyon.fr

§Project & Service Engineer, MicrodB, arthur.finez@microdb.fr,

¶Assistant Professor, quentin.leclere@insa-lyon.fr,

al.⁸ and Lewy⁹ using analytical formulations of the sound field in turbofan inlets. Farassat et al.¹⁰ have also presented a study of external mode detection using a single rotating arm.

On the other hand, pressure fluctuations sensed by in-duct wall-flush mounted microphones have a strong broadband component associated to the TBL hydrodynamic noise. While at tonal frequencies the aero-acoustic sound radiated by the machine is considerably higher than the hydrodynamic noise, this is not the case in the broadband part of the spectrum. Thus, a very low signal-to-noise ratio is observed away from tonal frequencies. For this reason, the application of modal decomposition techniques for the broadband component is more cumbersome for this configuration of microphone arrays.

In this paper we present the identification of the modal content associated to a small-scale ducted fan using two microphone array configurations. A first one with only wall-flush mounted microphones, installed downstream of the fan; and a second one with both an external array and a wall-flush mounted array upstream of the fan. The modal identification is applied for both tonal and broadband components of the noise radiated by the fan over a wide frequency range. The originality of this work consists first in introducing an optimized regularization procedure in the inverse mode decomposition technique and second in providing a direct comparison of internal and external mode decomposition results.

II. Theoretical background

The acoustic pressure inside an infinite cylindrical duct with hard walls may be expanded as follows (using cylindrical coordinates):¹¹

$$p(z, r, \phi) = \sum_{m=-\infty}^{\infty} \sum_{n=0}^{\infty} \left[A_{m,n} e^{-j k_{m,n}^+ z} + B_{m,n} e^{j k_{m,n}^- z} \right] f_{m,n}(r) e^{j m \phi}, \quad (1)$$

with $A_{m,n}$ and $B_{m,n}$ the complex coefficients of modes propagating downstream and upstream respectively. The subscripts m and n are the azimuthal and radial mode indices and $f_{m,n}(r)$ is a modal shape factor. It is assumed here that only cut-on modes contribute to the summation in (1), as if measurements are carried out relatively far from the source or any duct irregularity. The terms $k_{m,n}^{\pm}$ are the axial wavenumbers in downstream (+) and upstream (-) directions and are given by:

$$k_{m,n}^{\pm} = -\frac{M_z}{\beta^2} k_0 \pm \hat{k}_{r,m,n}, \quad (2)$$

with $M_z = U_0/c$ the Mach number along the z direction, $\beta^2 = 1 - M_z^2$ and $k_0 = \omega/c$ the wave number. The term $\hat{k}_{r,m,n}$ is given by:

$$\hat{k}_{r,m,n} = \frac{1}{\beta^2} \sqrt{k_0^2 - \beta^2 k_{r,m,n}^2}, \quad (3)$$

where $k_{r,m,n}$ stands for the value of k_r corresponding to the n th root of the equation:

$$J'_m(k_r r_0) = 0, \quad (4)$$

with $J'_m(\cdot)$ the first derivative of the m th order Bessel function $J_m(\cdot)$ and r_0 the duct internal radius. Assuming that K measurement positions are used to spatially sample the acoustic pressure inside the duct, one may write Eq. (1) in a matrix form:

$$\mathbf{p} = \mathbf{\Phi} \mathbf{c}, \quad (5)$$

with $\mathbf{p} \in \mathbb{C}^K$ a vector of complex measured pressure at a given frequency ω and $\mathbf{c} \in \mathbb{C}^L$ a vector containing the complex modal coefficients $A_{m,n}$ and $B_{m,n}$. The dimension L depending on the number of considered azimuthal (M) and radial (N) modes. The matrix $\mathbf{\Phi} \in \mathbb{C}^{K \times L}$ is filled with the corresponding terms of the modal basis. This linear system of equations may be solved for the coefficients \mathbf{c} as

$$\hat{\mathbf{c}} = \mathbf{\Phi}^\dagger \mathbf{p}, \quad (6)$$

where the superscript \dagger stands for the pseudo-inverse of a matrix. One alternative formulation may be used by defining the cross-spectral matrix of measurements as $\mathbf{S}_{\mathbf{p}\mathbf{p}} \triangleq \mathbb{E}\{\mathbf{p}\mathbf{p}^H\}$. Where the operator $\mathbb{E}\{\cdot\}$ should be understood as the expected value over the number of snapshots, as obtained by segmenting the time signal into short-time blocks then Fourier transforming. Equation (5) then reads

$$\mathbf{S}_{\mathbf{p}\mathbf{p}} = \mathbf{\Phi} \mathbf{S}_{\mathbf{c}\mathbf{c}} \mathbf{\Phi}^H, \quad (7)$$

and the solution is now written for the covariance matrix of the modal coefficients:

$$\hat{\mathbf{S}}_{\text{cc}} = \mathbf{\Phi}^\dagger \mathbf{S}_{\text{pp}} (\mathbf{\Phi}^\dagger)^H. \quad (8)$$

The above solution is suitable only if matrix $\mathbf{\Phi}$ is well-conditioned. However, this is not the case as the number of cut-on modes is increased (i.e. the frequency increases) and the matrix $\mathbf{\Phi}$ becomes ill-conditioned. In this case, one has to introduce *a priori* information into the problem in order to find a more stable solution. One example of such *a priori* information may be on the the energy of the solution. The idea is to penalize solutions having a high energy, what is mathematically translated by the Tikhonov regularization. First of all, we may conveniently express $\mathbf{\Phi}$ by its singular value decomposition:

$$\mathbf{\Phi} = \mathbf{U}[\mathbf{S}]\mathbf{V}^H. \quad (9)$$

The regularized inverse of $\mathbf{\Phi}$ in the sense of Tikhonov is then expressed as:

$$\mathbf{\Phi}^{\dagger R} = \mathbf{V} \left[\frac{s_i}{s_i^2 + \eta^2} \right] \mathbf{U}^H. \quad (10)$$

where $[a_i]$ symbolizes a diagonal matrix with generic diagonal element a_i and η^2 is a regularization parameter. The main difficulty of Tikhonov regularization is to optimally and automatically tune the parameter η^2 . Remember that it is often the case in acoustics that Eq. (8) is solved independently for each frequency over a wide frequency band. Several *ad hoc* methods were proposed for this task, for instance the L-curve¹² and GCV¹³ commonly used in acoustics. In this work use has been made of a method derived from a Bayesian approach of the inverse problem. It has been shown recently that this approach has several advantages as compared to traditional methods when applied to the inverse problems in acoustics.^{14,15} The approach boils down to the minimization of the following cost function with respect to η^2 :

$$\mathbf{J}(\eta^2) = \sum_{i=1}^I \ln(s_i^2 + \eta^2) + (I - 2) \ln \left(\frac{1}{I} \sum_{i=1}^I \frac{|y_i|^2}{s_i^2 + \eta^2} \right), \quad (11)$$

where the term $|y_i|^2$ stems from a projection of measurements onto the array subspace and is given by:

$$|y_i|^2 = \mathbf{u}_i^H \mathbf{S}_{\text{pp}} \mathbf{u}_i, \quad (12)$$

with \mathbf{u}_i the i th column of matrix \mathbf{U} . The minimization of the 1-D cost function in (11) is easily carried by evaluating it for a grid of potential values for η^2 and selecting the one that gives the minimum value for the cost function.

The same procedure described above may be applied for the modal identification using an external array at the vicinity of the fan inlet. The only difference is in the propagation model which relates the measurements to the modal amplitudes. Each acoustic mode emanating from the fan is conducted towards the duct termination, one part of the energy is reflected back and the other part radiates into the surroundings. A specific radiation pattern is associated to each acoustic mode, which generates a specific trace at the outside microphones. In this work, a commercial FEM solver is used to numerically compute the modal transfer matrix or directivity matrix.⁵ At a specific frequency, a computation is carried out for each mode as presented on figure 1(a-c). The computations are 2D axisymmetric. It can be seen from figures 1(a) and 1(b) that the duct has a focusing effect raising the pressure level at the center of the array. This is confirmed by the experimental measurements, as presented in figure 1(d), that shows the pressure levels at the microphone array for the first blade passing frequency. Figure 1(c) shows the computation for the mode (0,3). This mode is cut-off in the duct at the first Blade Passing Frequency so the pressure amplitudes are very low at the array position. Such cut-off modes are ignored in the computations. This modal identification approach is tested on a ducted fan configuration encountered in air conditioning systems of aircrafts. The experimental set-up is presented in the next section.

III. Experimental set-up

III.A. Description of the ducted fan system

The test bench is constituted of a ducted air conditioning fan which is illustrated in Figure 2(a). The fan has 17 blades and 23 Outlet Guide Vanes (OGV). This machine has the particularity that 3 out of the 23

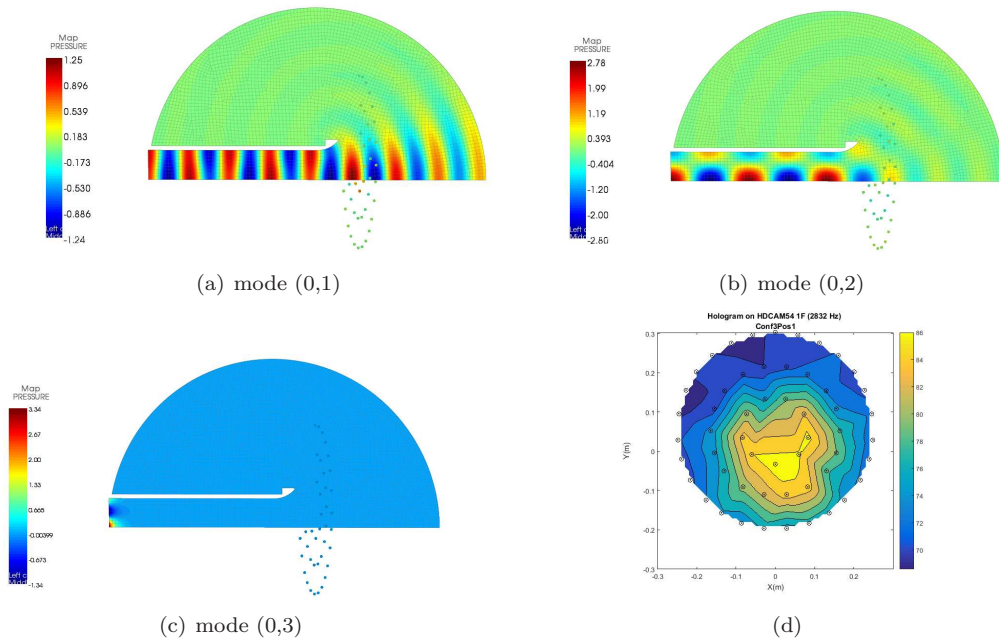


Figure 1. (a-c) Numerical computation for different modes at the 1st BPF (2833 Hz). (d) Hologram (pressure levels) at 2833 Hz (1st BPF) measured on the array from the experiment.

stator vanes are thickened due to structural reasons. In the downstream direction, the fan casing is extended by an aluminum straight circular duct of the same diameter and 2m long. This in order to prevent the array microphones from contamination by cut-off modes. Those modes are indeed expected to be limited to the vicinity of the fan. At the nominal rotation speed of 10000 rpm, the Blade Passing Frequency (BPF) and first harmonics are 2833 Hz, 5666 Hz and 8500 Hz. The duct diameter is 17cm and the installation was not equipped with a turbulence control screen (TCS).

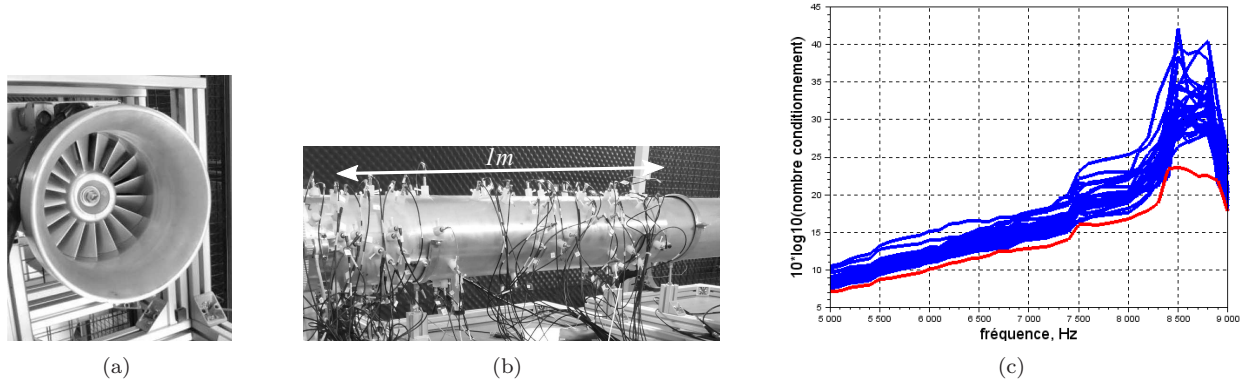


Figure 2. (a) Front view of the tested fan installed in a 17cm diameter duct. (b) Picture of the wall-flush mounted microphone array placed about 2m downstream the fan-OGV system. (c) Array positioning optimization using the transfer matrix condition number. Among many microphone positioning (blue curves) the one with the lowest condition number is selected (red curve).

III.B. Downstream wall-flush mounted microphone array

The array illustrated on Figure 2(b) is constituted of two sub-arrays where microphones are flush-mounted on the duct inner surface so as to do not disturb the flow. The first one is defined here as Large Random Array (LRA): it is 80 cm long in the axial direction and constituted of 53 microphones. The second one is named Small Random Array (SRA): it is 20 cm long and also constituted of 53 microphones. All the 106 microphones are 1/4 in. Bruel & Kjaer of types 4957 and 4958. They are connected to a 128-channels acquisition system and the sampling frequency is set to 65536 Hz. The microphones are mounted on the duct inner surface using a *pin-hole* system (see appendix of Salze *et al.*¹⁶). The modification of the microphone

frequency responses due to this type of mounting is taken into account by a calibration procedure using an artificial acoustic source.¹⁷

The positioning of microphones has been optimized to ensure the best performance in the mode decomposition procedure. This is achieved by testing a large number of microphone positioning sets and computing the transfer matrix for each configuration. The array with the lowest condition number on the whole frequency range (100-10000 Hz) is then selected as shown in Figure 2(c).

III.C. Upstream wall-flush mounted array and external planar array

In this configuration, a commercially available 54-microphones planar array is placed in front of the inlet and a 53-microphones wall flush mounted array is placed just upstream of the fan (see Figure 3). The acquisition is made simultaneously for both arrays and allows a direct comparison between modal decomposition obtained by the two approaches.

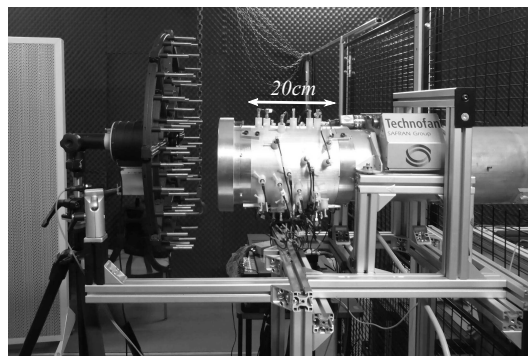


Figure 3. Picture of the external array in front of the fan inlet and the upstream wall-flush mounted array.

The transfer matrix between the modal amplitudes and the pressure values at the microphone location determines the ability of the method to perform the modal identification. For the external microphone array, the transfer matrix is computed numerically and relates the amplitudes of upstream propagating modes to the radiated acoustic pressure at the microphone positions. On the other hand, for the in-duct microphone array the analytical basis presented in equation (1) is used with both downstream and upstream propagating modes. At the second blade passing frequency (5666Hz), the condition number of the numerical transfer matrix is 54. It should be compared to the condition number of the transfer matrix of the duct surface array which is 97. The lower condition number of the numerical transfer matrix can be explained by the fact that there is 2 times less modes to be identified as compared to the in-duct transfer matrix (described by both downstream and upstream propagating modes).

IV. Results

IV.A. Preliminary analysis

From the global parameters of the machine, the classical Tyler and Sofrin¹⁸ rule allows to determine the azimuthal periodicity of the acoustic modes produced at harmonics of the Blade Passing Frequency (BPF). This rule holds for perfectly axisymmetric inlet flows and regular OGV arrangements and designs. In the current case, the azimuthal mode orders at 1st BPF are $m = \dots, 17, -6, -29, \dots$; at 2nd BPF $m = \dots, 34, 11, -12, \dots$ and at 3rd BPF $m = \dots, 28, 5, -18, \dots$ all modes produced at 1st and 2nd BPF according to Tyler and Sofrin rule are naturally cut-off during their propagation in the duct as previously mentioned.¹ This means that tonal noise should not be heard at a sufficient distance from the fan at 1st and 2nd BPF (as long as the assumption of flow and geometric regularity holds). On the contrary, modes $m = 5$ are already cut-on at 8500 Hz (3rd BPF) so at this frequency rotor-stator interaction is expected to overtake the broadband phenomena in the far-field noise spectra.

The results presented on the following sections are obtained with the fan operating at its nominal speed, that is equal to 10000 rpm. Typical pressure spectral density measured at the microphone location are plotted on Figure 4. Strong tonal noise contribution on the first three 3 BPF's are clearly visible at 2833 Hz, 5666 Hz and 8500 Hz. As previously commented, contribution at BPF 1 and 2 are not expected and

clearly exhibit a violation of the regularity/homogeneous assumption. This could be due either to an inlet flow distortion (turbulence ingestion noise) or to the fact that stator vanes are not homogeneous (rotor wake-OGV interaction tonal noise). Additional noise pollution by the turbulent boundary layer (TBL) developed on the duct wall is also visible on the auto-spectrum (black) with a SNR at the order of magnitude of about -10 dB.

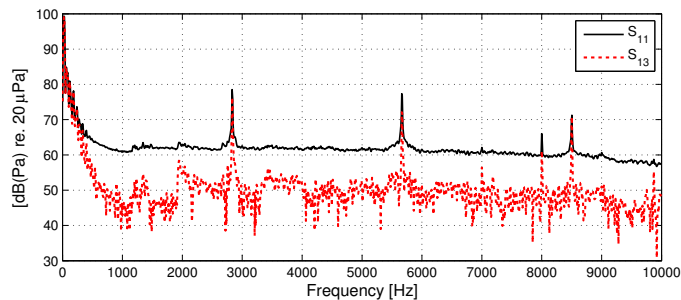


Figure 4. Example of measured in-duct acoustic pressure field. Solid black line: autospectrum of microphone nr. 1; dashed red line: cross-spectrum between microphones nr.1 and nr.3

IV.B. Tonal noise

In this section, modal identification results are presented at the tonal frequencies (corresponding to the BPF and its first 2 harmonics) for the two microphone array arrangements.

First of all, results are shown for the downstream wall-flush mounted microphone array. On Figures 5(a) and 5(d) the identified modal amplitudes at the first BPF are plotted as function of the mode indices (m,n) for both downstream and upstream propagation directions. It can be seen that downstream propagating modes are indeed more powerful than upstream propagating modes, indicating that most of the acoustic energy, at this frequency, is actually absorbed by the duct anechoic termination. Note that the downstream propagating mode (-3,0) is the most powerful.

Results for the second BPF are presented on Figures 5(b) and 5(e). One can see that the downstream propagating mode (-6,0) is the most energetic. According to the Tyler and Sofrin's rule, modes of azimuthal order $m = -6$ should not be generated by an homogeneous fan-OGV system, however, they are experimentally observed. Thus, it might be generated due to the heterogeneous OGV, since at this frequency modes ($\pm 6,0$) are cut-on both in the annular section and in the circular section, it is expected to be observed at the array position once excited.

For the third BPF the results are shown for both the regularized solution (see Figures 5(c) and 5(f)) and the non-regularized solution (see Figure 6). At this frequency, the number of modes to be identified is comparable to the number of microphones and the inversion of the modal matrix is ill-conditioned. It can be seen that for the non-regularized solution the amplitudes of upstream propagating modes (Figure 6(b)) are at the same order of magnitude as the downstream propagating modes (Figure 6(a)). This result is not intuitive, since one would expect the amplitudes of upstream propagating modes to be very low at this frequency, due to the duct anechoic termination. On the other hand, for the regularized solution the amplitudes of upstream propagating modes are much lower than those from downstream modes (see Figures 5(c) and 5(f)). A modal decomposition taking into account only downstream propagating modes has also been performed at this frequency. In this case, the number of unknowns is divided by two and the matrix to be inverted is not ill-conditioned. The obtained results were equivalent to those shown in Figure 5(c) and thus validates this regularized solution. Looking at the results in figure 5(c), among the most energetic modes we may highlight: the modes (5,0) and (5,1) which were expected according the Tyler and Sofrin rule as commented above; and a particularly powerful mode (9,0) which is not predicted by the theory. These experimental results could be directly compared with analytical studies dealing with the stator inhomogeneity (e.g. Roger and Caule¹).

In order to infer on the physical mechanisms at the origin of the observed modal coefficients we may evaluate their mutual coherence.^{5,6} The modal coherence between two modes c_{mn} and $c_{m'n'}$ can be calculated

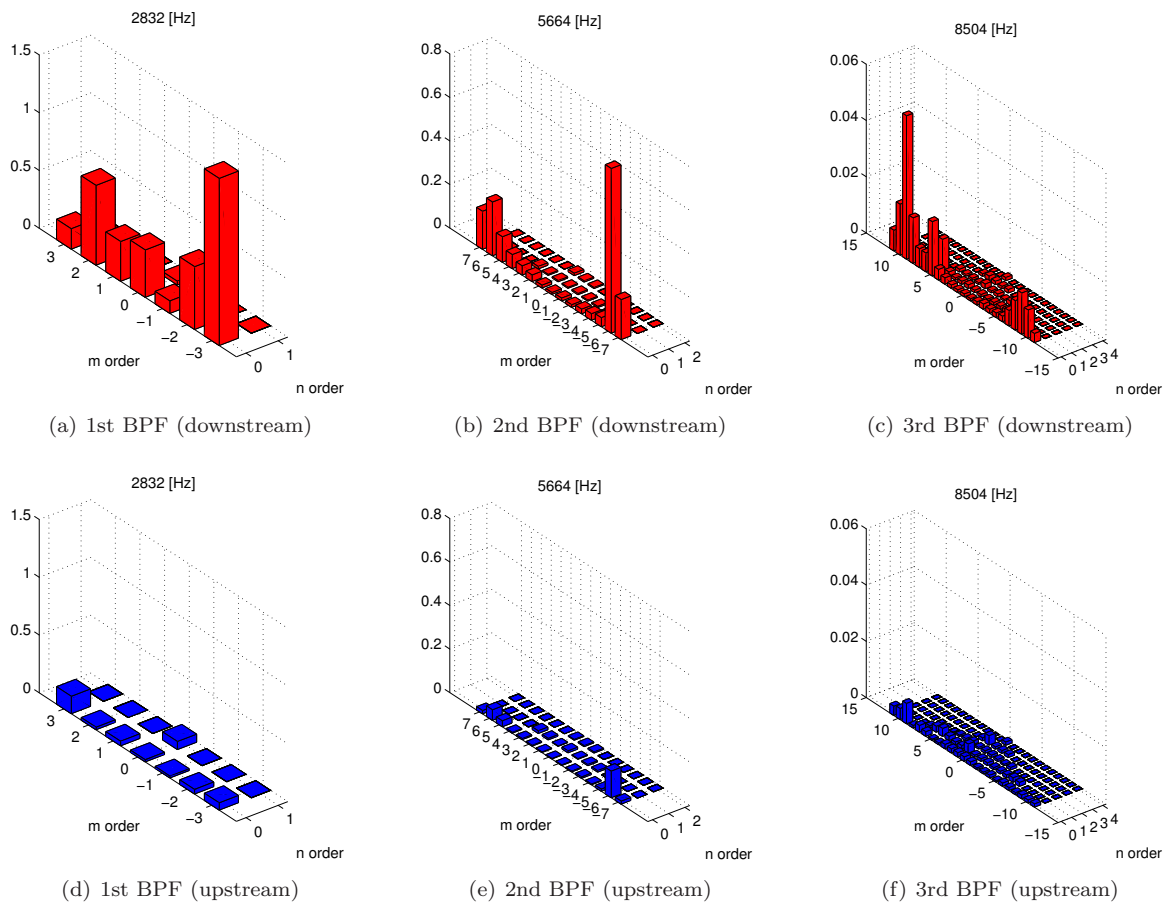


Figure 5. Modal decomposition obtained for the first 3 blade passing frequencies (BPF). Top row: downstream propagating modes; bottom row: upstream propagating modes. The same axis limits are used for both downstream and upstream propagating modes. m is the azimuthal order and n is the radial order starting from zero, such that the $(0,0)$ mode corresponds to a plane wave. Positive azimuthal orders corresponding to co-rotating modes. Results are shown in a linear scale.

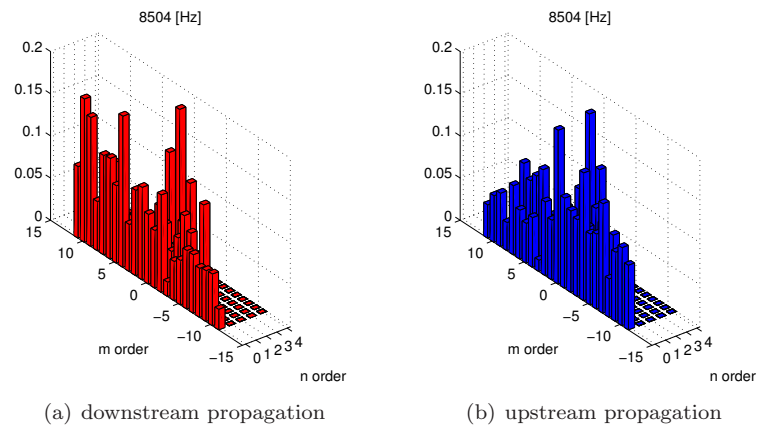


Figure 6. Modal decomposition at the fan's 3rd BPF, non-regularized solution.

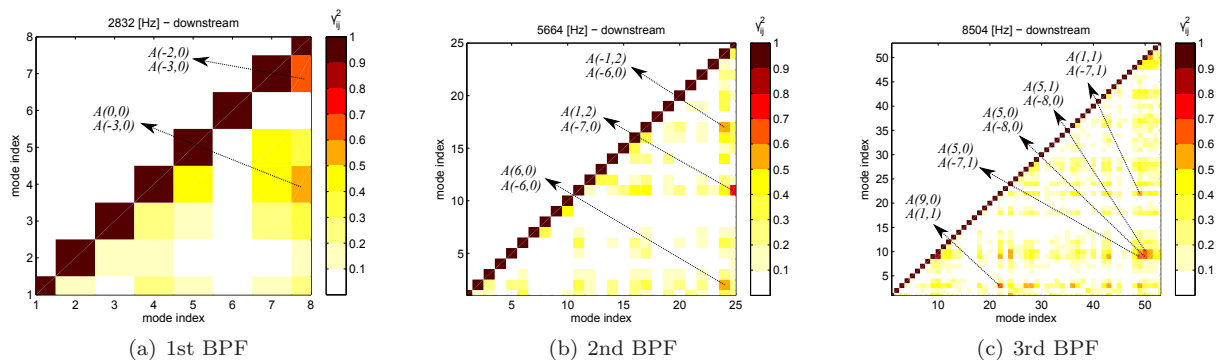


Figure 7. Coherence between modal coefficients obtained for the first 3 blade passing frequencies (BPF). Only coherence between downstream propagating modes are shown. Since the modal coherence matrix is symmetric, only its lower triangular part is shown. The diagonal represents the modal coherence of a mode with itself and is equal to one by definition. Coherence values range from 0 to 1.

from the covariance matrix of modal coefficients (see Eq. (8)) as follows:

$$\gamma_{c_{mn}c_{m'n'}}^2(\omega) = \frac{|\hat{S}_{c_{mn}c_{m'n'}}(\omega)|^2}{\hat{S}_{c_{mn}c_{mn}}(\omega)\hat{S}_{c_{m'n'}c_{m'n'}}(\omega)}, \quad (13)$$

where $\hat{S}_{c_{mn}c_{m'n'}}$ is the cross-spectrum between modes c_{mn} and $c_{m'n'}$ and $\hat{S}_{c_{mn}c_{mn}}$ the auto-spectrum of mode c_{mn} with m and n being the azimuthal and radial orders respectively. As pointed out by Castres and Joseph,⁵ the degree of coherence between two modes evaluated at tonal frequencies may be used to discriminate between rotor-stator interaction noise (for which one should expect a high degree of coherence) and noise issued from the interaction between upstream flow distortion and the fan blades. The modal coherence between cut-on modes are shown in Figure 7 for the first 3 BPF's. Looking at the mutual modal coherence for the 1st BPF, see Figure 7(a), it can be particularly seen that modes (-2,0) and (-3,0), and modes (0,0) and (-3,0) have a non-negligible coherence level. It can be argued thus that these modes are partially generated by a rotor-stator interaction. The same analysis has been done for the 2nd BPF, in this case it can be noticed particularly modes (1,2) and (-7,0) as well as modes (6,0) and (-6,0). In general, one can notice that the largest coherence values at the BPF and its first two harmonics are at the order of 60% to 70%. It can be argued that both mechanisms (i.e. inflow distortions and rotor-stator interaction) are contributing to the radiated noise at these tonal frequencies. In fact the experimental set-up was carried out without a turbulence control screen (TCS), it is thus likely that inflow distortions were present during measurements. A new TCS has been recently installed in the experimental test bench and it would be interesting to further investigate this subject.

Finally, results are presented for the configuration in which pressure signals are simultaneously measured by both an upstream in-duct array and an external array (see Figure 3). A comparison between the results of modal identification produced from both array data is provided in Figure 8. Notice that only amplitudes of upstream propagating modes are shown for the duct surface array for the sake of comparison. A good

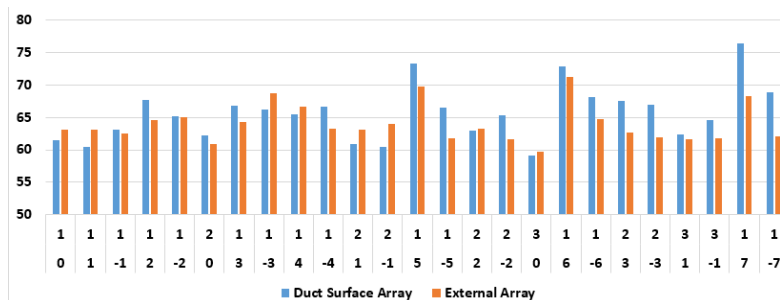


Figure 8. Modal coefficients shown in a dB scale at the 2nd BPF obtained by: upstream wall-flush mounted array (blue) and external array (orange). Notice that radial mode indices are starting from 1, such that the (0,1) mode corresponds to the plane wave.

agreement between the internal and external modal decomposition is found on Figure 8. Except for mode

(7,1) for which the estimated amplitude using the external array is about 8dB lower than the one obtained by the internal array. It may be due to a poorer azimuthal discretization of the external array as compared to the in-duct array.

The modal detection technique using an external array has proven to be feasible using a numerical solver to compute the scattering effect of the inlet mouth. Some drawbacks have been identified namely the intrusive character of the upstream array. A better radial discretization is provided by the external array. However, with the current microphone arrangement, a possible lack of azimuthal discretization has been identified. To go further, a numerical study and a microphone location optimization procedure could help to clarify this situation. Another possible work extension would be to take into account few cut-off modes in the model, to separate out this additional pollution which can be significant for the closest microphones to the fan.

IV.C. Broadband noise

In this section modal identification results are presented for the broadband component of the noise radiated by the ducted fan. As discussed in Section I, broadband modal identification from in-duct pressure microphones is more cumbersome (as compared to the tonal part) due to the contamination by the turbulent boundary layer noise. In order to illustrate the interest on the application of cross-spectral matrix denoising techniques,¹⁹ an example is taken at two different frequencies in the broadband region (5000 Hz and 6504 Hz).

First of all, it is shown in Figure 9 the identified modal coefficients that were obtained by processing the original (noisy) CSM, that is, with both the acoustical and hydrodynamic components. It can be seen that the dynamic range^a of identified coefficients is at the order of 8 dB. Thus the method cannot separate modes with amplitude less than 8dB from the higher mode, they are seen as “noise”.

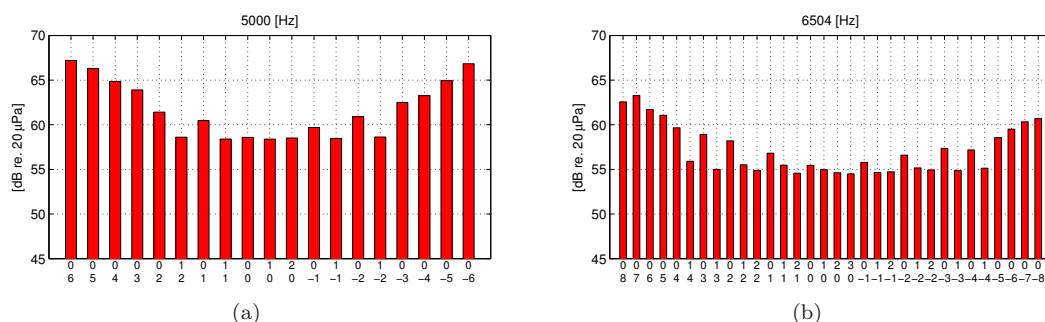


Figure 9. Modal decomposition in the broadband part of the spectrum for two different frequencies: (a) 5000 Hz; (b) 6504 Hz. These results were obtained with the raw (noisy) cross-spectral matrix. Results are shown in a dB scale.

A first attempt to improve this results is to simply set the diagonal of the CSM to zero (diagonal removal technique). The identified modal coefficients are shown in Figure 10. Notice that results are now presented in a linear scale and show both downstream and upstream propagating modes. It can be seen that the results are not satisfactory, modes with negative autopower (which have no physical meaning) are identified.

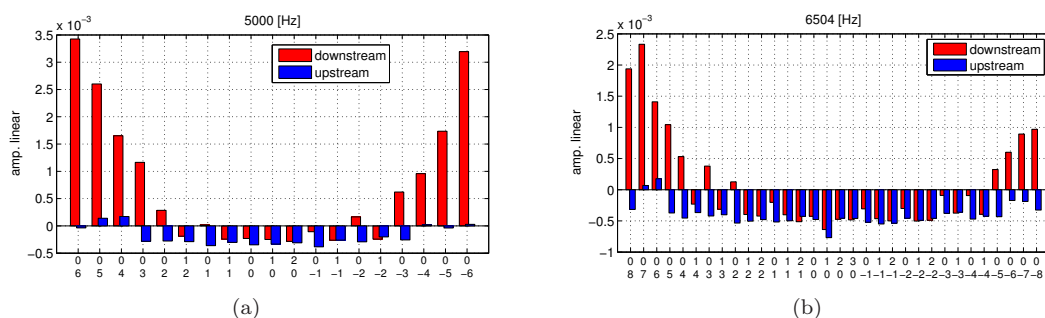


Figure 10. Modal decomposition in the broadband part of the spectrum for two different frequencies: (a) 5000 Hz; (b) 6504 Hz. These results were obtained with the cross-spectral matrix with diagonal removal. Results are shown in a linear scale.

^aThe dynamic range is represented here by the difference in amplitude between the most energetic mode and the plateau at the noise floor.

The denoising approach based on the decomposition of the CSM into low-rank and sparse parts¹⁹ is then applied. Modal coefficients estimated by processing this “cleaned” CSM are shown in Figure 11. We can notice that no negative auto-powers are observed and by looking on the results in a dB scale (see Figure 12), the dynamic range is now at the order of 14 dB (gain of around 6dB as compared to the noisy CSM). These results are computed for narrow-band frequencies, one could expect that results averaged over 3rd octave bands could exhibit even better performance.

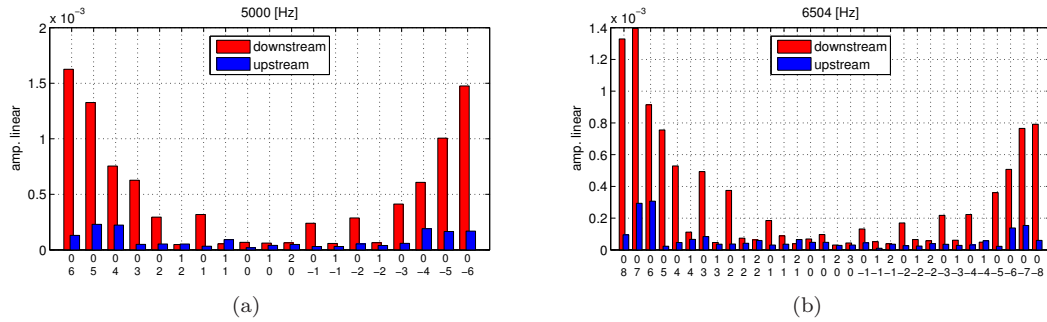


Figure 11. Modal decomposition in the broadband part of the spectrum for two different frequencies: (a) 5000 Hz; (b) 6504 Hz. These results were obtained with the denoised cross-spectral matrix using a technique presented in ref.¹⁹ Results are shown in a linear scale.

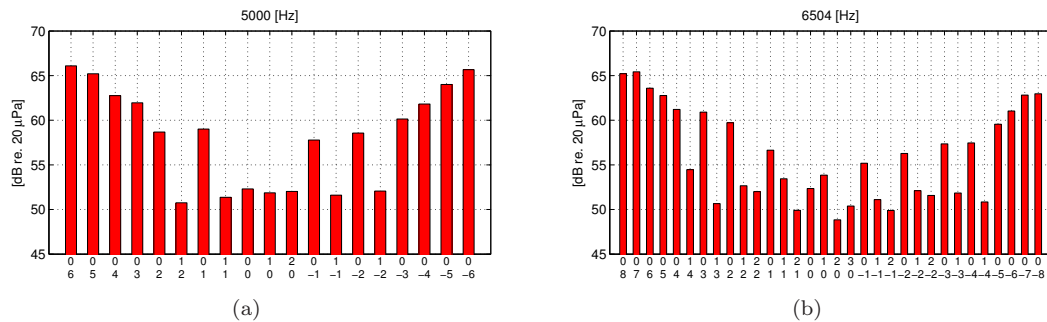


Figure 12. Modal decomposition in the broadband part of the spectrum for two different frequencies: (a) 5000 Hz; (b) 6504 Hz. These results were obtained with the denoised cross-spectral matrix using a technique presented in ref.¹⁹ Results are shown in a dB scale.

Finally, estimated modal coefficients integrated over 3rd octave frequency bands are shown in Figure 13. The modal coefficients at the tonal frequencies have not been taken into account in the average. It can be observed from these results a tendency of higher levels towards co-rotating modes (positive spinning orders m). This observation is in agreement with those found in an experimental test with a Boeing 18-inch fan rig in the Boeing Low-Speed Aeroacoustic Facility (LSAF).²⁰ Although, in this experimental set-up the in-duct microphone array was positioned either in the inlet (upstream of the fan) or in the aft duct (between the rotor and the stator).

V. Conclusion

This paper illustrates some applications of modal identification for the characterization of the acoustic sources of a ducted fan. The modal decomposition is realized from in-duct measurements in downstream and upstream directions, and from external measurements, using a numerical model. Results in the upstream direction for in-duct and external measurements are in good agreement. It is also shown that at higher frequencies (i.e. when the number of modes to be identified is comparable to the number of microphones) a regularization procedure is necessary to stabilize the inversion of the modal matrix.

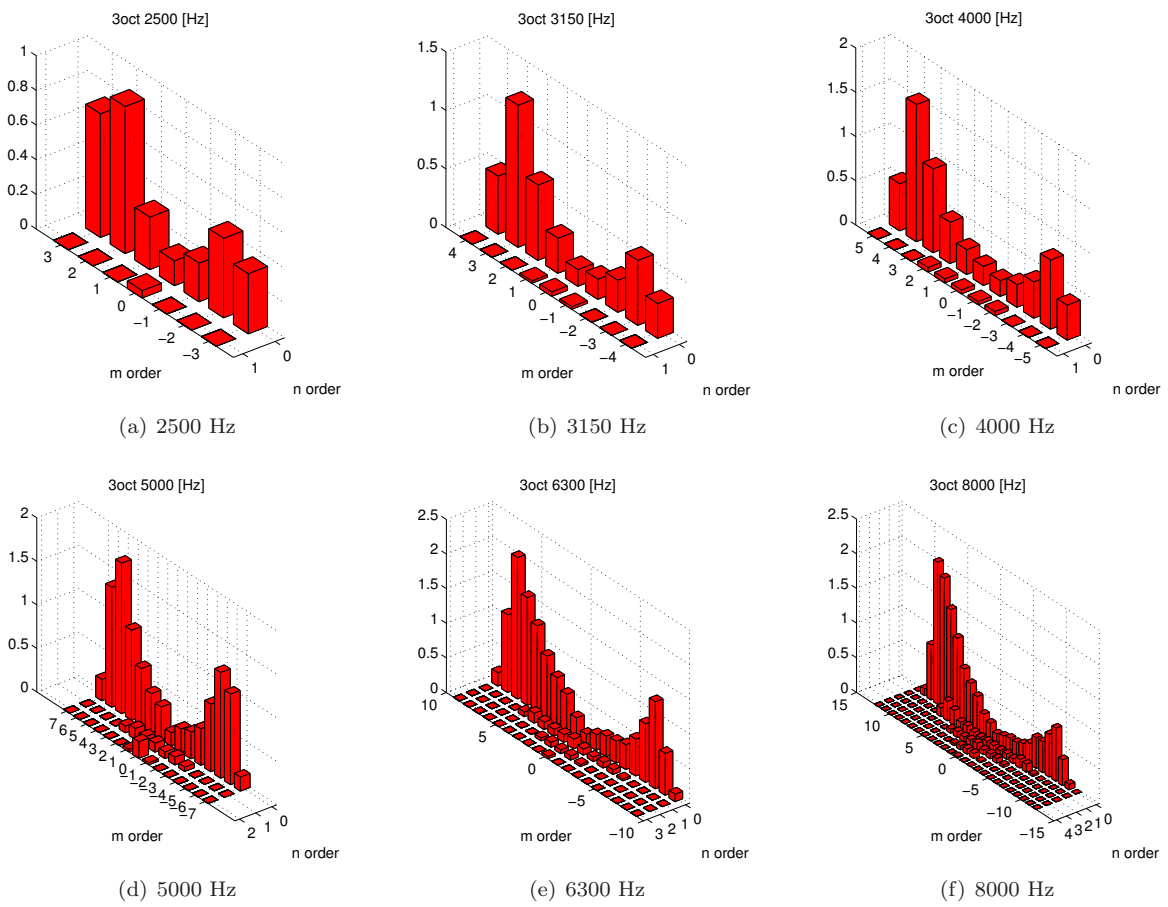


Figure 13. Broadband modal coefficients averaged over third octave frequencies. Both azimuthal (m) and radial (n) mode indices are represented. Positive azimuthal orders corresponding to co-rotating modes. Results are shown in a linear scale.

Acknowledgments

This work is supported by the FRAE in the French program SEMAFOR. It has been performed within the framework of the Labex CeLyA of Université de Lyon, operated by the French National Research Agency (ANR-10-LABX-0060/ ANR-11-IDEX-0007) and supported by the Labcom P3A (ANR-13-LAB2-0011-01). The authors would like to thank Jean-Michel Perrin for setting up the experiment and Simon Bouley for his help during the experimental campaign.

References

- ¹Roger, M. and Caule, P., “Assessment of the Effect of Stator Inhomogeneity on Rotor-Stator Tonal Noise,” *15th International Symposium on Transport Phenomena and Dynamics of Rotating Machinery, ISROMAC-15, Honolulu, HI*, 2014.
- ²Bouley, S., François, B., Roger, M., Posson, H., and Moreau, S., “On a mode-matching technique for sound generation and transmission in a linear cascade of outlet guide vanes,” *21st AIAA/CEAS Aeroacoustics Conference, Dallas, USA, 2015*, No. 2825, 2015.
- ³Roger, M., Moreau, S., and François, B., “Towards Cascade Trailing-Edge Noise Modeling Using a Mode-Matching Technique,” *21st AIAA/CEAS Aeroacoustics Conference, Dallas, USA, 2015*, No. 2541, 2015.
- ⁴Enghardt, L., Neuhaus, L., and Lowis, C., “Broadband sound power determination in flow ducts,” *10th AIAA/CEAS Aeroacoustics Conference*, American Institute of Aeronautics and Astronautics, 2004, AIAA 2004-2940.
- ⁵Castres, F. O. and Joseph, P. F., “Experimental investigation of an inversion technique for the determination of broadband duct mode amplitudes by the use of near-field sensor arrays,” *The Journal of the Acoustical Society of America*, Vol. 122, No. 2, 2007, pp. 848–859.
- ⁶Bennett, G. J., O’Reilly, C., Tapken, U., and Fitzpatrick, J., “Noise source location in turbomachinery using coherence based modal decomposition,” *Proceedings of the 15th AIAA/CEAS Aeroacoustics Conference, Miami, FL, USA*, No. 3367, 2009.
- ⁷Tapken, U., Raitor, T., and Enghardt, L., “Tonal Noise Radiation From an UHBR Fan - Optimized In-Duct Radial Mode Analysis,” *Proceedings of the 15th AIAA/CEAS Aeroacoustics Conference, Miami, FL, USA*, No. 3288, 2009.
- ⁸Castres, F., Joseph, P., and Astley, R., “Mode detection in turbofan inlets from acoustic pressure measurements in the radiated field,” *10th AIAA/CEAS Aeroacoustics Conference*, American Institute of Aeronautics and Astronautics, 2004, Volume: 2004-2953.
- ⁹Lewy, S., “Inverse method predicting spinning modes radiated by a ducted fan from free-field measurements,” *The Journal of the Acoustical Society of America*, Vol. 117, No. 2, 2005, pp. 744–750.
- ¹⁰Farassat, F., Nark, D. M., and Thomas, R. H., “The Detection of Radiated Modes From Ducted Fan Engines,” *7th AIAA/CEAS Aeroacoustics Conference, Maastricht, The Netherlands, 2001*, No. 2138, 2001.
- ¹¹Munjaj, M., *Acoustics of Ducts and Mufflers With Application to Exhaust and Ventilation System Design*, Wiley-Interscience publication, Wiley, 1987.
- ¹²Hansen, P. C. and O’Leary, D. P., “The use of the L-curve in the regularization of discrete ill-posed problems,” *SIAM J. Sci. Comput.*, Vol. 14, November 1993, pp. 1487–1503.
- ¹³Golub, G. H., Heath, M., and Wahba, G., “Generalized Cross-Validation as a Method for Choosing a Good Ridge Parameter,” *Technometrics*, Vol. 21, No. 2, 1979, pp. 215–223.
- ¹⁴Antoni, J., “A Bayesian approach to sound source reconstruction: Optimal basis, regularization, and focusing,” *The Journal of the Acoustical Society of America*, Vol. 131, No. 4, 2012, pp. 2873–2890.
- ¹⁵Pereira, A., Antoni, J., and Leclère, Q., “Empirical Bayesian regularization of the inverse acoustic problem,” *Applied Acoustics*, Vol. 97, 2015, pp. 11 – 29.
- ¹⁶Salze, E., Bailly, C., Marsden, O., Jondeau, E., and Juvé, D., “An experimental characterization of wall pressure wavevector-frequency spectra in the presence of pressure gradients,” *20th AIAA/CEAS Aeroacoustics Conference, Atlanta, GA*, No. 2909, 2014.
- ¹⁷Leclère, Q., Pereira, A., Finez, A., and Souchotte, P., “Indirect calibration of a large microphone array for in-duct acoustic measurements,” *Journal of Sound and Vibration*, 2016, accepted for publication.
- ¹⁸Tyler, M. and Sofrin, T. G., “Axial Flow Compressor Noise Studies,” *Society of Automotive Engineers Transactions*, Vol. 70, 1962, pp. 309–332.
- ¹⁹Finez, A., Pereira, A., and Leclère, Q., “Broadband noise decomposition of ducted fan noise using spectral-matrix denoising,” *Proceedings of Fan Noise 2015, Lyon, France*, 2015.
- ²⁰Ganz, U. W., Joppa, P. D., Patten, T. J., and Scharpf, D. F., “Boeing 18-Inch Fan Rig Broadband Noise Test,” Tech. Rep. CR-1998-208704, NASA, 1998.